Biomass burning emissions from satellite observations: synergistic use of formaldehyde (HCHO), fire counts and surface temperature.

Thierry Marbach[a], Steffen Beirle[a], Cheng Liu[a], Ulrich Platt[b], Thomas Wagner[a]
[a]Max-Planck Institut for Chemistry, J.J. Becher Weg 27, 55128 Mainz, Germany;
[b]Institut of Environmental Physics, INF 229, 69120 Heidelberg, Germany

ABSTRACT

Satellite observations provide unique opportunities for the identification of trace gas sources on a global scale. We present case studies for the synergistic use of satellite observations by comparing formaldehyde (HCHO) time series with fire count measurements as well as with surface temperature to identify the tropospheric sources of HCHO. The fire counts and temperature are taken as proxy for biomass burning events and vegetation activity, respectively. Both are sources of HCHO, either direct or trough photochemical oxidation of non-methane hydrocarbons (e.g. biogenic isoprene emissions). Formaldehyde time series are derived from satellite observations made by the GOME instrument. This instrument provides almost 8 years of continuous HCHO global observations, which constitute an ideal case to calculate time series over specific regions for various trace gases.

Nine regions have been selected to investigate the influence of fire counts (biomass burning proxy) and the temperature (vegetation activity proxy) on the HCHO tropospheric columns. The chosen time series has a length of 6 years (from July 1996 to June 2002). The results show that biogenic sources of HCHO are in many cases the strongest HCHO sources. For example over south east of the USA, the correlation with temperature was very high indicating a strong biogenic source of HCHO (through isoprene emissions). The biomass burning source typically shows more pronounced seasonal patterns or is even of sporadic nature. Over the Amazon region, the correlation with fires is high indicating that in this area most of the HCHO is caused by biomass burning. In several other regions for both sources moderate correlation coefficients were found.

Keywords: Formaldehyde (HCHO), Biomass Burning, Vegetation, Satellite Remote Sensing.

1. INTRODUCTION

We already know from the emission inventories for various trace gases the possible and expected sources. However, for many trace gases, these estimates are still subject to large uncertainties. One particular problem is that in many cases trace gas emissions from different sources are mixed, especially if they are located close to each other (e.g. biomass burning and biogenic emissions as sources for HCHO). In such cases the identification of the source of tropospheric trace gases is still a big challenge. The comparison of the trace gases results with observations from other satellite instruments (like e.g. fire counts) allows to constrain more precisely the identification of different trace gas sources.

As a principal intermediate in the oxidation of hydrocarbons in the troposphere, formaldehyde (HCHO) is an important indicator of tropospheric hydrocarbon emissions and photochemical activity. The global atmospheric HCHO 'background' originates mainly from the oxidation of methane (CH_4) by the hydroxyl radical (OH) in most of the troposphere; loss of HCHO occurs by photolysis and reaction with OH or by wet removal. Additional, locally, HCHO sources are primary emission product from biomass burning and from fossil fuel combustion [1]. Moreover, HCHO is formed in the atmosphere as an intermediate in the photochemical oxidation of non-methane hydrocarbons from biogenic or anthropogenic sources (mainly isoprene and alkenes) [2]. Due to the rather short lifetime of HCHO of a few hours [3], HCHO proves to be an important indicator of local sources, e.g. biogenic emissions, biomass burning [4, 5], and industrial activities (oxidation of non-methane hydrocarbons an also HCHO emissions in solvent and wood industry) over continents. In fact, while the oxidation of the relatively constant atmospheric CH_4 concentration also leads to a rather constant background concentration of HCHO, these additional sources cause 'anomalies' in the HCHO distribution [6, 7, 8, 9].

Remote Sensing of Fire: Science and Application, edited by Wei Min Hao,
Proc. of SPIE Vol. 7089, 70890J, (2008) · 0277-786X/08/$18 · doi: 10.1117/12.793654

Analyzing long time series of satellite measurements provides unique opportunities for the identification and the characterization of trace gas sources on a global scale. Using our improved GOME (Global Ozone Monitoring Experiment) retrieval for formaldehyde [10] we process an almost 8 year (January 1996 to June 2003) time series of daily maps of the global formaldehyde distribution (full coverage at the equator is achieved within 3 days). From these measurements, a variety of details of the HCHO distribution can be investigated ranging from strong signals of biogenic emissions and biomass burning to rather weak signals e.g. over some industrialized regions or ship tracks [10, 11, 12, 13, 14]. Some of the observed patterns show a very regular occurrence, while also some episodic events (e.g. caused by ENSO) are found [15, 16].

2. METHOD

2.1 HCHO GOME retrieval

The Global Ozone Monitoring Experiment instrument (GOME, launched in 1995 onboard ERS-2) is a nadir viewing spectrometer observing the UV/visible spectral range continuously between 240 and 790 nm at a moderate spectral resolution from 0.2 to 0.4 nm [Burrows et al., 1999a]. It measures the solar irradiance and the upwelling earthshine radiance. The satellite operates in a near-polar, Sun-synchronous orbit at an altitude of 780km with a local equator crossing time at approximately 10:30. The typical ground pixel size is 40km (along track i.e. approximately north-south) times 320km (across-track i.e. approx. east-west). Each across-track scan is divided in three pixels (west, centre, east pixel). The coverage of the whole surface of the Earth takes three days at the equator with improving sampling towards higher latitudes (daily coverage for the polar region). A key feature of GOME is its ability to detect not only ozone but also several other chemically active atmospheric trace gases such as NO_2, SO_2, BrO, H_2O, OClO and HCHO by means of Differential Optical Absorption Spectroscopy (DOAS; [17, 18]). Compared to other trace gas absorptions (e.g. ozone or NO_2), the HCHO absorption seen by GOME is typically rather weak (of the order of 0.1% optical density (OD)). In addition, in the spectral window of the HCHO retrieval (about 337 – 360nm), several other trace gases (O_3, BrO, NO_2, O_4) show also substantial absorption features, making the retrieval a difficult task. Thus we performed a rather sophisticated DOAS retrieval, which is described in detail below.

First we perform an independent spectral calibration of the satellite spectra. This calibration is based on the fitting of a highly resolved solar spectrum, convoluted with the satellite slit function, to the satellite spectra. The resulting accuracy of the spectral calibration is of the order of 0.01nm. A particular advantage is that the spectral calibration is determined directly from the measured satellite spectra. Using this spectral calibration, the trace gas cross sections (HCHO, BrO, NO_2) are convoluted to the instruments spectral resolution. Note that for O_3 instead an interpolation is performed, because the used O_3 cross sections (at 221 K and 241 K) were measured by the GOME instrument itself [19]; also O_4 is interpolated, because the spectral features of the spectrum are wider than the spectral resolution of the GOME instrument). In addition to the absorption spectra, also a Ring spectrum is prepared; it is calculated from a direct solar measurement [20, 21]. In this way a consistent set of reference spectra is prepared, which is the prerequisite to minimize the spectral interference between the HCHO absorptions with other absorbers (in particular ozone). During the spectral DOAS retrieval, all reference spectra are allowed to 'shift' in wavelength to correct for possible instrumental changes. However, 'shift' of all spectra is linked to those of the Fraunhofer reference spectrum. For the Fraunhofer reference spectrum an average of several earth shine spectra selected on a daily basis over the central Pacific (175°E, 145°W, 20°N, 20°S) is used. This region is usually not affected by strong sources of HCHO and the location is symmetrical to the equator to minimize seasonal effects. Using this Fraunhofer reference spectrum instead of the direct sun measurement, overcomes the problem caused by the GOME diffuser plate [22, 23].

For the GOME observations we found that the retrieved HCHO absorptions show a systematic dependence on the viewing angle of the instrument: for the different GOME ground pixels (east, centre, west) slight, systematic offsets were found, which can not be explained by the atmospheric distribution of HCHO or the dependence of the absorption path on the viewing angle. The reason for these offsets is still not completely understood. Possible causes are the systematic dependencies of the Ring effect and the degree of polarization on the viewing angle. While this effect is still under investigation, currently we apply a pragmatic solution to correct for these offsets: we selected two spectra (east and west pixel) over regions without significant HCHO absorption. The ratio spectrum of these two spectra is also included as a artificial cross-section in the fitting routine. This technique almost completely removes the artificial east-west differences. In this study, we only consider (almost) cloud free pixels, i.e., the cloud fraction (taken from the Heidelberg

Iterative Cloud Retrieval Utilities HICRU [24] being less than 5%. The result of the spectral DOAS analysis is the slant column density (SCD, the trace gas concentration along the atmospheric light paths) of HCHO. The stratospheric HCHO can be neglected. Thus, the retrieved slant columns directly represent the tropospheric HCHO.

2.2 Additional datasets

The GOME cloud free (less than 5% cloud cover) HCHO SCDs have been compared to two other datasets in order to determine the importance of biogenic emissions and the biomass burning as HCHO source. The additional datasets are fire counts (data from "ATSR World Fire Atlas", from the Data User Element of the European Space Agency: http://dup.esrin.esa.int/ionia/wfa/) and 2 meter surface temperature (data from ERA40 of the European Centre for Medium-Range Weather Forecasts, ECMWF, database: http://data.ecmwf.int/data/). The fire counts and the 2 meter surface temperature are used as biomass burning and "vegetation" proxy, respectively. It has to be noted that the GOME overpass local time is 10:30, so the closest ECMWF data have been taken at 12:00. The time difference to the ATSR dataset is about half a day because the the ATSR instrument (also onboard ERS-2) is measuring during the night time. The three datasets (GOME HCHO SCDs, ATSR fire counts and ECMWF surface temperatures) have a common time overlap of 6 years, from July 1996 to June 2002. This period has been chosen to calculate time series of each datasets.

2.3 Studied regions

Table 1. Description of the 9 selected boxes.

Box name	Localization	HCHO SCD values	Fire count intensities	Remark
USA S-E	40°N; 30°S -95°W; -80°E	Moderate	Low	Forest cover with little fires
Amazon	0°N; -19°S -70°W; -45°E	Very high	High	Mostly Evergreen forest with strong seasonal biomass burning events
Amazon N-W	0°N; -5°S -80°W; -62°E	Very high	Very low	Evergreen forest area with very less fire counts compared to the neighboring Amazon box
Africa center 1	10°N; 5°S -15°W; 10°E	Very high	Low to moderate	Forest cover with moderate seasonal biomass burning events
Africa center 2	10°N; 5°S 10°W; 40°E	Moderate	High	Forest cover with strong seasonal biomass burning events
Africa S-W	-4°N; -11°S 10°W; 30°E	Very high	High	Forest cover with strong seasonal biomass burning events
Asia S-E	23°N; 12°S 92°W; 106°E	High	Moderate	Punctual strong and/or seasonal moderate biomass burning events
Indonesia	5°N; -8°S 97°W; 119°E	High	High	Punctual intense biomass burning events over evergreen forest region
Australia N	-12°N; -20°S 122°W; 146°E	Low	High	Strong seasonal biomass burning events over a non forest region

In many cases both sources (biomass burning and biogenic emissions) are situated at the same area. Figure 1a shows a mean multiyear HCHO SCD map (January to June 2003) compared to the fire count location (from July 1996 to June 2003) and with a MODIS land cover map of 2001 (http://edcdaac.usgs.gov/modis/mod12c1v4.asp). Three main HCHO sources are situated along the equator, over regions covered by evergreen forest (Amazon basin, Africa and Indonesia). But these regions regularly also experience strong biomass burning events. Weaker HCHO sources can also be observed

over the south east of the USA, over Mexico, Europe, Africa, Madagascar, India and in south east Asia and northern part of Australia. In those regions the biomass burning show different levels of intensity. To study in more detail the influence of biogenic and biomass burning emissions as source for tropospheric HCHO, we choose 9 regions with different characteristics (summarized in table 1 and displayed on figure 1).

3. RESULTS AND DISCUSSION

3.1 Description of the time series

The calculated time series (July 1996 to June 2002) for the three datasets (GOME HCHO SCD, ATSR fire counts, ECMWF surface temperature) are displayed in figure 2 and 3 for each selected box described in section 2.3.

In the USA S-E box we see a high seasonal temperature amplitude in phase with a seasonal HCHO SCD variability (summer months). The fire counts are low.

The Amazon box displays low temperature amplitude but seasonally high biomass burning events in coincidence with maximum HCHO SCDs (autumn months).

In Amazon N-W the temperature amplitude is small and the fire counts are very low. The HCHO SCDs are very high like in the neighboring Amazon box.

The Africa center 1 results show moderate seasonal biomass burning events during winter time as well as moderate temperature amplitude. The HCHO SCDs also has a seasonal variation.

In Africa center 2 box the seasonal biomass burning events are high in winter time (as for Africa box 1). The temperature variation is also similar to the Africa box 1, but the HCHO SCDs do not displayed a regular variability.

Africa S-W box shows regular seasonal biomass burning (summer month) with a maximum slightly shifted by 1-2 months compared to the HCHO SCD maximum (end of summer). The temperature amplitude is small.

In the Asia S-E box the fire activity is regularly zero during the summer months but preceded by fires in spring. The temperature amplitude is low and the HCHO SCDs time series show no clear variability scheme.

The Indonesia box displays one high biomass burning events with two peaks during autumn 1997 and spring 1998. This increase in fire detection corresponds to the particularly strong El-Niño climatic event of 1997-1998. Dryer conditions around the Pacific Ocean have induced strong biomass burning over Indonesia, Central America, and in the eastern part of Siberia [15, 16]. The temperature amplitude is small and the HCHO SCD variability does not show a clear scheme.

Australia N shows a seasonally occurring biomass burning during the end of summer. The temperature amplitude displays higher temperatures in winter and lower in summer (southern hemisphere). Here also the HCHO SCD variability does not display a clear scheme that could be explained by the fire counts or the temperature.

3.2 Biomass burning and temperature correlation with HCHO SCDs

In order to have a better understanding of the relation between the time series, we performed correlation analyze of the time series of monthly mean values for the different regions. The resulting correlation coefficients are presented in Figure 4.

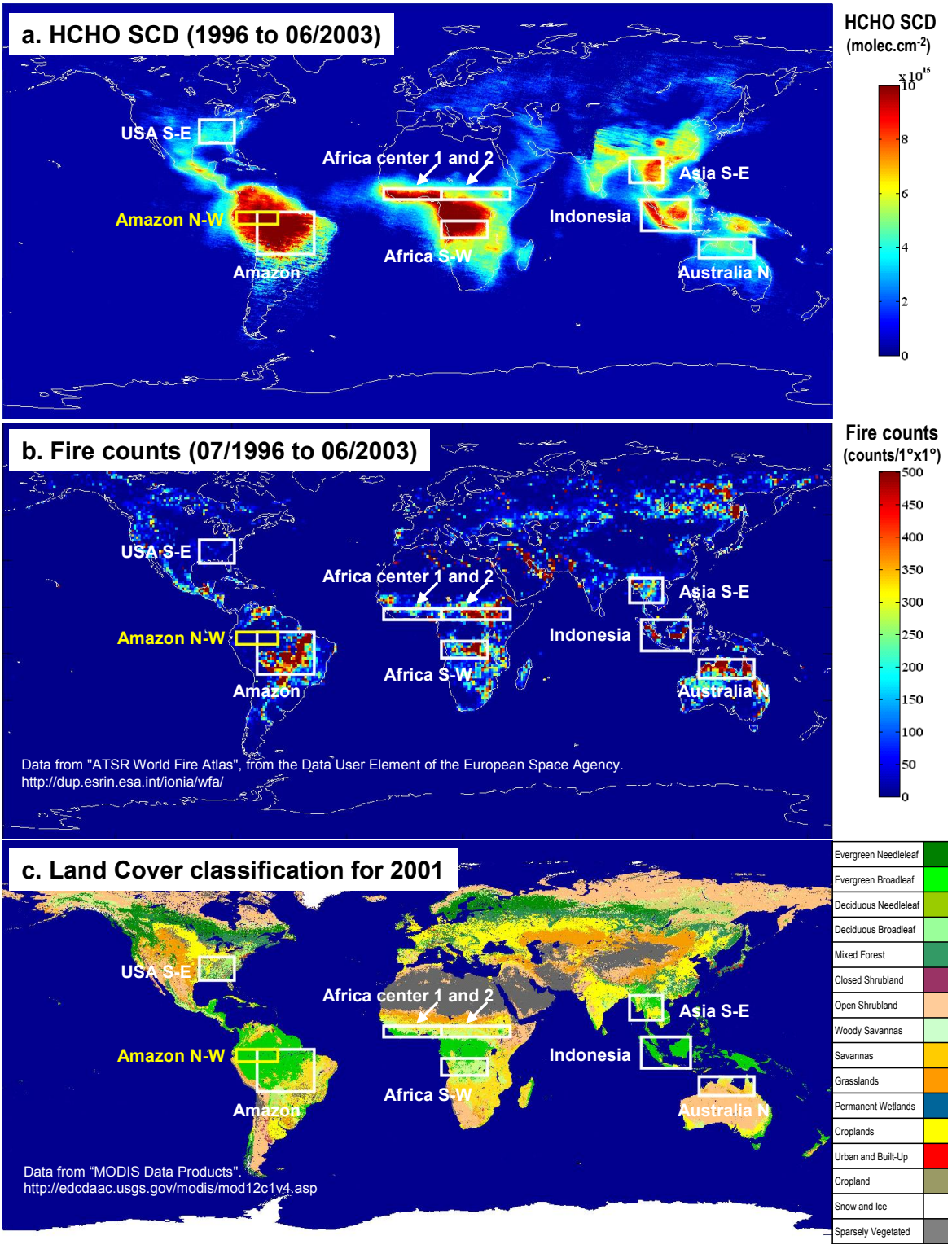

Fig. 1. Location of the 9 selected boxes for the comparison of HCHO columns (a), the fires counts (b), and the land cover (c). The Amazon N-W region (yellow box) has been used to investigate a 'fire free' region close to a region with intense fire events (Amazon box).

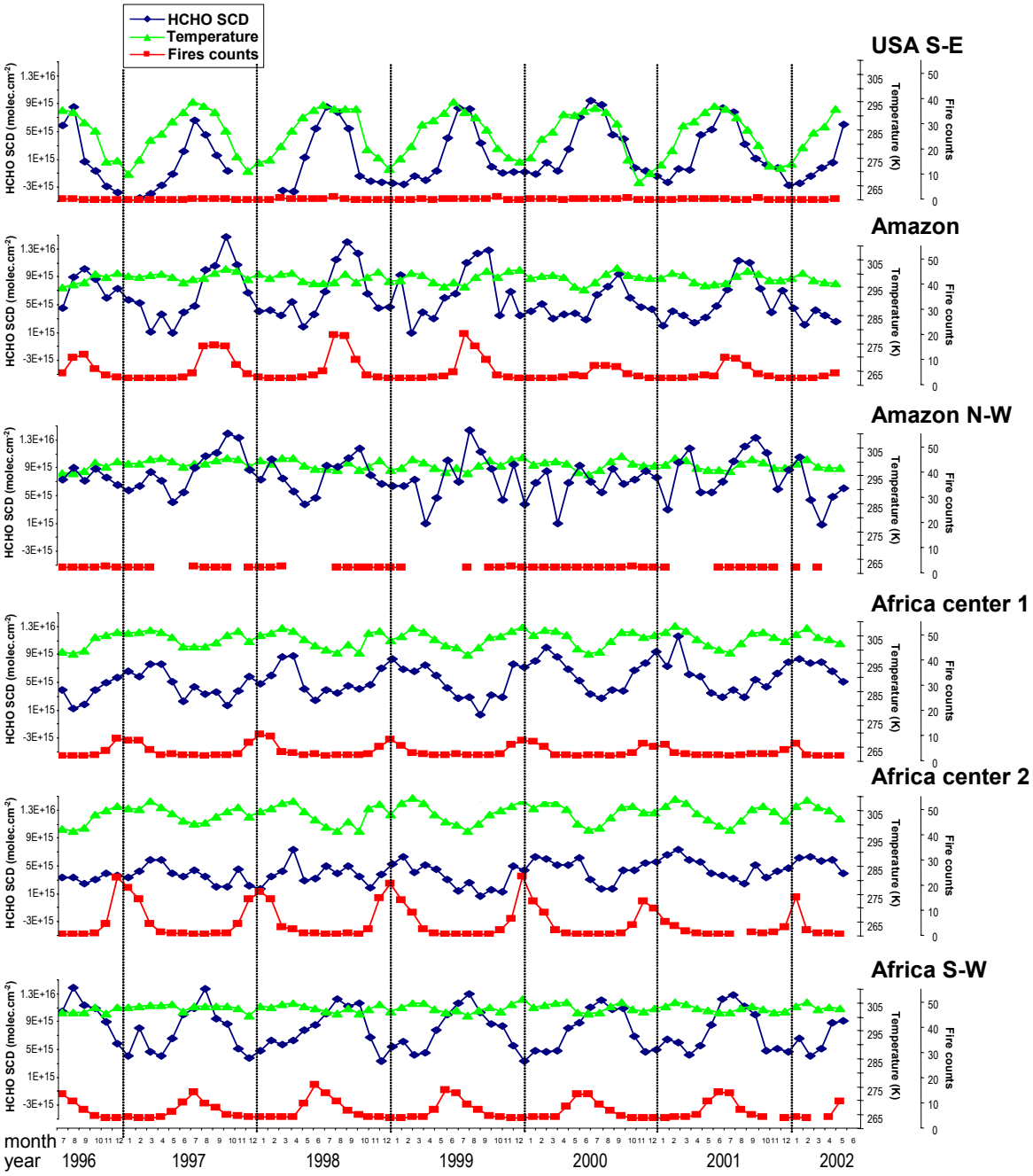

Fig. 2. HCHO SCD, temperature and fire time series from July 1996 to June 2002 (in America and Africa regions). For all similar plots the same scale has been used in order to allow a direct comparison between the different regions. The gaps in fire counts and in HCHO SCD are caused by no fire detection and too high retrieval errors, respectively.

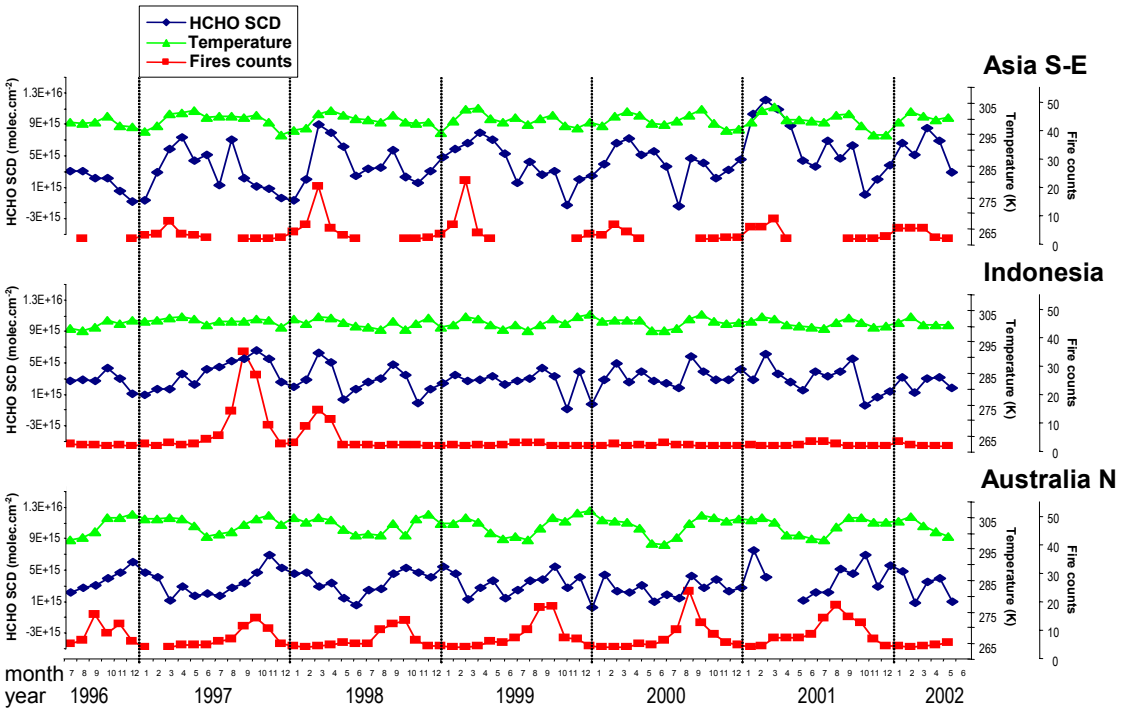

Fig. 3. HCHO SCD, temperature and fire time series from July 1996 to June 2002 (in Asia, Indonesia and Australia regions). For all similar plots the same scale has been used in order to allow a direct comparison between the different regions. The gaps in fire counts and in HCHO SCD are caused by no fire detection and too high retrieval errors, respectively.

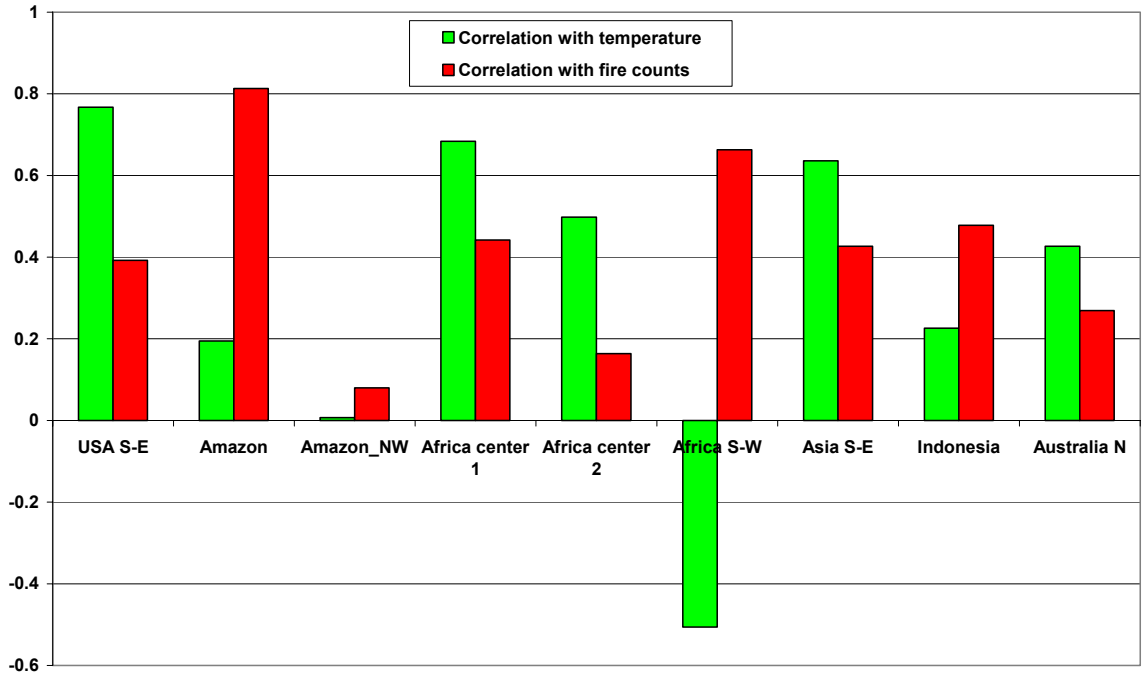

Fig. 4. Correlation coefficients for the temperature and the fire count time series to the HCHO SCDs time series.

For the USA S-E box the correlation coefficients confirm the relation between temperature and HCHO SCDs seen in Figure 2. The correlation with fires is not negligible and can be explained by punctual high biomass burning events. If the temperature time series is taken as proxy for the vegetation influence, this result is in agreement with previous studies [12, 13].

The Amazon box shows a high correlation with the fire counts (also seen in Figure 2). The correlation is low with the temperature. In this region the biomass burning emissions seem to represent a strong source of tropospheric HCHO.

The Amazon N-W region displays correlation neither with fire counts nor with the temperature. The no-correlation with biomass burning was expected from low fire counts. The no-correlation with the temperature could be explained from the low temperature amplitude, but is still a surprising result that should be investigated in a further study.

Africa center 1 and 2 show surprising results. Although in both regions strong and regular biomass burning occurs, the correlation is even higher with the temperature, particularly for Africa center 1 which has the highest HCHO SCDs. This behaivior is so far not well understood. Possibly, it is related to the high correlation between the temperature and the fires themselves.

The Africa S-W region also displays unexpected results. The correlation with fires is high and a little bit smaller with the temperature. The correlation with fires is in agreement with the seasonal variations of fire counts and HCHO SCDs seen in figure 2. The unexpected negative correlation with the temperature might be related to the very weak amplitude of the temperature variations in this region.

In the Asia S-E area the correlation with temperature is high. The correlation with fires is much smaller and probably reflects the spring biomass burning events shown in figure 3.

Indonesia shows moderate correlation with fire counts and low correlation with temperature. The punctual but intense biomass burning event (e.g. due to ENSO) can explain the correlation to the fire counts.

For Australia N moderate correlation with temperature is found. Surprising is the rather low correlation with fire counts because Figure 3 displays seasonally strong fire counts. This finding should be investigated in more detail in the future.

4. CONCLUSIONS AND OUTLOOK

The biogenic sources of HCHO are in many cases the strongest HCHO sources and show no strong variation (e.g. over evergreen forest). The biomass burning source typically shows more pronounced seasonal patterns or is even of sporadic nature. In order to decompose the contributions from biogenic emissions and biomass burning, we investigated the time series of monthly mean values for selected regions of the world. Besides the satellite measurements of HCHO, we also calculated the time series for fire counts (from ATSR) and the surface temperature (from ECMWF data). The fire counts and temperature data can be seen as proxies for the biomass burning emissions and biogenic emissions. From the correlation analyses between HCHO data with the other data sets we derived information on the importance of both sources for the different regions. In some cases (e.g. south east of the USA) the correlation with temperature was very high indicating a strong biogenic source of HCHO (through isoprene emissions). In contrast, in other regions, the correlation with fire counts is high (e.g. over the Amazon region) indicating that in this area most of the HCHO is caused by biomass burning. In several other regions for both sources moderate correlation coefficients were found. For Amazon N-W, low correlation coefficients for both sources were derived, which should be investigated in a further study.

While the results of these simple correlation analyses are already very promising, in the future several improvements should be made:

a) it has to be clarified, for which regions the temperature is a suitable proxy for the biogenic emissions,

b) possibly the biogenic emissions can be also (and probably much better) quantified by observations of the vegetation index; also for satellite observations of such indices the correlation coefficients should be determined,

c) besides determining the correlation coefficients for individual pairs of data sets, multi-correlation analyses should be performed, including e.g. also possible linear trends,

d) In addition to the different possible emission sources, also the influence of transport processes as well as aerosols effects should be investigated,

e) finally, atmospheric model results should be also compared to the satellite data sets of HCHO. Such a comparison will allow a much more comprehensive characterization and quantification of the various sources of HCHO.

In addition we plan to compare the satellite observations of HCHO also to other trace gases measured from satellite instruments. CO as proxy for fires counts [25] will have the advantage to have the measurement at a similar local time instead of an half day shift (ATSR and AATSR are made during the night time of the satellite orbit, GOME during the daytime). Also NO_2 is emitted from biomass burning but not to biogenic emissions.

Our studies will also benefit from the better temporal and regional resolution of GOME 2 (launched onboard of METOP in October 2006). These would improve our knowledge of the influence of biomass burning and biogenic emissions on the chemistry and evolution of the atmosphere.

ACKNOWLEDGEMENTS

The German Research Foundation (DFG) and ACCENT-TROPOSAT-2 are gratefully acknowledged for financial support. ESA is also thanked for providing the ERS-2 data.

The fire counts data have been downloaded from the data user element of the European Space Agency "ATSR World Fire Atlas", http://dup.esrin.esa.int/ionia/wfa/

The 2 meter surface temperature have been downloaded from the European Centre for Medium-Range Weather Forecasts ECMWF, http://data.ecmwf.int/data/

The MODIS map has been downloaded from the NASA webpage: http://edcdaac.usgs.gov/modis/mod12c1v4.asp.

REFERENCES

[1] Anderson, L. G., Lanning, J. A., Barrel, R., Mityagishima, J., Jones, R. H., and Wolfe, P., "Sources and sinks of formaldehyde and acetaldehyde: An analysis of Denver's ambient concentration data," Atmospheric Environment, 30, 2113-2123 (1996).

[2] Meller, R., Moortgat, G. K., "Temperature dependence of the absorption cross sections of formaldehyde between 223 and 323 K in the wavelenght range 225-375 nm," Journal of Geophysical Research, 105, 7089-7101 (2000).

[3] Arlander, D. W., Brüning, D., Schmidt, U., and Ehhalt, D. H., "The Tropospheric Distribution of Formaldehyde During TROPZ II, Journal of Atmospheric Chemistry," 22, 251-268 (1995).

[4] Carlier, P., Hannachi, H., and Mouvier, G., "The chemistry of carbonyl compounds in the atmosphere," Atmospheric Environment, 20, 2079-2099 (1986).

[5] Lipari, F., Dasch, J. M., and Scuggs, W. F., "Aldehyde emissions from wood-burning fireplaces," Environment Sciences Technology, 18, 326-330 (1984).

[6] Lee, Y.-N. and al., "Atmospheric chemistry and distribution of formaldehyde and several multioxygenated carbonyl compounds during the 1995 Nashville/Middle Tennessee Ozone Study," Journal of Geophysical Research, 103, 22449-22462 (1998).

[7] Munger, J. W., Jacob, D. J., Daube, B. C., Horowitz, L. W., Keene, W. C., Heikes, B. G., "Formaldehyde, glyoxal. and methylglyoxal at a rural mountain site in central Virginia," Journal of Geophysical Research, 100, 9325-9334 (1995).

[8] Altshuller, A. P., "Production of aldehydes as primary emissions and from secondary atmospheric reactions of alkenes and alkanes during the night and early morning hours, Atmospheric Environment," 27, 21-31 (1993).

[9] Levi, H., "Normal atmosphere: Large radical and formaldehyde concentrations predicted," Sciences, 173, 141-143 (1971).

[10] Marbach, T., Beirle, S., Platt, U., Hoor, P., Wittrock, F., Richter, A., Grzegorski, M., Vrekoussis, M., Burrows, J., and Wagner t., "Satellite Measurements of Formaldehyde from Shipping Emissions," Submitted to ACP (2008).

[11] Wittrock, F., A. Richter, H. Oetjen, J. P. Burrows, M. Kanakidou, S. Myriokefalitakis, R. Volkamer, S. Beirle, U. Platt, and T. Wagner, "Simultaneous global observations of glyoxal and formaldehyde from space," Geophys. Res. Lett., 33, L16804, doi:10.1029/2006GL026310 (2006).

[12] Palmer, P. I., Abbot, D. S., Fu, T-M., Jacob, D. J., Chance, K., Kurosu, T., Guenther, A., Wiedinmyer, C., Stanton, J., Pilling, M., Pressley, S., Lamb, B., and Sumner, A. L., "Quantifying the seasonal and interannual variability of North American isoprene emissions using satellite observations of formaldehyde column," J. Geophys. Res., doi:10.1029/2005JD006689 (2006).

[13] Chance, K., Palmer, P. I., Spurr, R. J. D., Martin, R. V., Kurosu, T. P., and Jacob, D. J., "Satellite observations of formaldehyde over North America from GOME," Geophysical Research Letters, 27, 3461-3464 (2000).

[14] Thomas, W., Hegels, E., Slijkhuis, S., Spurr, R., and Chance, K., "Detection of biomass burning combustion products in Southeast Asia from backscatter data taken by the GOME spectrometer," Geophys. Res. Lett. 25, 1317-1320 (1998).

[15] Marbach, T., Beirle, S., Frankenberg, C., Platt, U. and Wagner, T., "Identification of tropospheric trace gas sources: synergistic use of HCHO and other satellite observations," ESA publication SP-636, ISBN 92-9291-200-1 (2007).

[16] Spichtinger, N., Damoah, R., Eckhardt, S., Forster, C., James, P., Beirle, S., Marbach, T., Wagner, T., Novelli, P., and Stohl, A., "Boreal forest fires in 1997 and 1998: a seasonal comparison using transport model simulations and measurement data, Atmospheric Chemistry and Physics," Vol. 4,1857-1868 (2004).

[17] Platt, U., "Differential optical absorption spectroscopy (DOAS), in Air Monitoring by Spectroscopic Techniques," Chem. Anal. Ser., 127, 27-84 (1994).

[18] Platt, U., and Stutz, J., "Differential Optical Absorption Spectroscopy Principles and Applications. Series: Physics of Earth and Space Environments," Springer, 597 p., ISBN: 978-3-540-21193-8 (2008).

[19] Burrows, J. P., Dehn, A., Deters, B., Himmelmann, S., Richter, A., Voigt, S., and Orphal, J., "Atmospheric Remote-Sensing Reference Data from GOME: 2." Temperature-Dependent Absorption Cross Sections of O_3 in the 231-794 nm Range, Journal of Quantitative Spectroscopy and Radiative Transfer, 61, 509-517 (1999b).

[20] Solomon, S., Schmeltekopf, A. L., and Sanders, R. W., "On the interpretation of zenith sky absorption measurements," J. Geophys. Res. 92, 8311-8319 (1987).

[21] Bussemer, M., "Der Ring-Effekt, „Ursachen und Einfluß auf die spektroskopische Messung stratosphärischer Spurenstoffe," Diploma thesis, University of Heidelberg (1993).

[22] Richter, A., and Wagner, T., "Diffuser Plate Spectral Structures and their Influence on GOME Slant Columns," Technical Note (2001).

[23] Richter, A., and Burrows, J., "Retrieval of Tropospheric NO_2 from GOME Measurements," Adv. Space Res. 29 (11), 1673-1683 (2002).

[24] Grzegorski, M., Wenig, M., Platt, U., Fournier, N., Stammes, P., and Wagner, T., "The Heidelberg iterative cloud retrieval utilities (HICRU) and its application to GOME data," Atmos. Chem. Phys., 6, 4461-4476 (2006).

[25] Liu, C., Penning de Vries, M., Beirle, S., Hoor, P., Marbach. T., Frankenberg, C., Platt, U., Wagner, T., "Relationship between ATSR fire counts and CO vertical column density retrieved from SCIAMACHY onboard ENVISAT," submitted to SPIE Optics (2008).